

# Holocene lake level variations on the Qinghai-Tibetan Plateau

Xiang-Jun Liu · Zhong-Ping Lai · Fang-Ming Zeng ·  
David B. Madsen · Chong-Yi E

Received: 10 December 2012 / Accepted: 24 March 2013 / Published online: 11 April 2013  
© Springer-Verlag Berlin Heidelberg 2013

**Abstract** Paleoshorelines indicative of multiple high lake stages can be found around many lakes on the Qinghai-Tibetan Plateau (QTP). Conspicuous paleoshorelines associated with the most recent highstands can be readily observed on satellite images and during field investigations. However, earlier paleoshorelines have been identified at only a few sites around these lakes due to a lack of clear shoreline features and limited spatial extension of those that can be identified. We investigated past lake highstands using published chronologies, Aster-DEM, Google Earth, and ArcGIS 9.2 software. These data suggest that (1) paleoshorelines of the most recent lake highstand were formed during the Holocene; (2) during this highstand, lake levels reached more than 90, 60–90, and 30–60 m higher than present in the central Gangdise and

western Qiangtang areas, while in the eastern Qiangtang, Holxil-Yushu, and northeastern QTP areas highstands did not exceed 30 m above modern; (3) during the early Holocene, some lakes on the southwestern QTP combined to form large lakes, while lakes in the inland areas of the QTP were only a little larger during the Holocene high lake level stages.

**Keywords** Paleoshorelines · Holocene lake level variations · Qinghai-Tibetan Plateau (QTP)

## Introduction

A “shoreline” is the land margin of a large body of water (such as an ocean, sea, or lake) that has been geologically modified by the action of water, while a “beach” is a shoreline feature composed of water-modified sand, gravel, pebbles, or cobblestones (<http://en.wikipedia.org/wiki/Shore>). Paleoshorelines were formed when detrital sediments (sand and gravel) were sufficient and lake levels were reasonably stable during different stages of lake evolution (Stapor 1982; Chen 1986; Lee et al. 2009; Li et al. 2009). They represent past lake areal extensions and lake level elevations. Beach ridges and their subsurface deposits thus record past coastal processes and are indicators of past shoreline positions and shapes (Tamura 2012). Paleoshorelines represent past lake levels that are critical for the understanding of lake–climate interaction, sediment production and delivery, and tectonic uplift of the Tibetan Plateau (Li et al. 2009). However, most observable paleoshorelines provide a biased record since they tend to be the product of recent regressive phases, with older shorelines more likely to have been erased during repeated transgressive–regressive lake level fluctuations (Li 2000; Lee et al. 2009).

**Electronic supplementary material** The online version of this article (doi:10.1007/s00531-013-0896-2) contains supplementary material, which is available to authorized users.

X.-J. Liu · Z.-P. Lai · F.-M. Zeng · D. B. Madsen  
Key Laboratory of Salt Lake Resources and Chemistry, Qinghai  
Institute of Salt Lakes, Chinese Academy of Sciences, Xining  
810008, China

X.-J. Liu (✉)  
Key Laboratory of Tibetan Environment Changes and Land  
Surface Processes, Institute of Tibetan Plateau Research,  
Chinese Academy of Sciences, Beijing 100085, China  
e-mail: xjliu@isl.ac.cn

D. B. Madsen  
MOE Key Laboratory of West China’s Environmental System,  
Research School of Arid Environment and Climate Change,  
Lanzhou University, Lanzhou 730000, China

C.-Y. E  
School of Life and Geographic Science, Qinghai Normal  
University, Wusi Road, Xining, China

On high-resolution satellite images, most lakes, as well as many currently dry closed-basins, on the Qinghai-Tibetan Plateau (QTP) appear to be surrounded by conspicuous regressive shoreline rings attesting to high water levels in the past (Avouac et al. 1996; Li 2000). Due to both tectonic movements and multiple climate change cycles, the lakes on the QTP experienced multiple high lake stages during the Quaternary (Chen 1986; Li 2000). Earlier shorelines have been damaged by subsequent geomorphological processes and we have found remnant older shorelines sporadically distributed in only a few places around the lakes using both satellite images and field investigations (Li 2000; Zheng et al. 2006; Meng et al. 2012). The conspicuous shoreline features around QTP lakes are thought to have formed during the last lake regression phase (Li 2000), with the implication that the climate gradually became drier subsequently (Chen 1986).

Direct numerical dating of shoreline deposits has variously shown that QTP lakes experienced high levels during marine isotope stage (MIS) 5 (Zhao et al. 2003; Zhu et al. 2005; Yang et al. 2006; Madsen et al. 2008; Fan et al. 2010; Liu et al. 2010), MIS 3 (Li 2000; Jia et al. 2001; Shi et al. 1999, 2001), the last deglaciation (Wang and Shi 1992; Li et al. 2001; Kong et al. 2007) and the Holocene (Gasse et al. 1991; Fontes et al. 1996; Lee et al. 2009; Xue et al. 2010; Liu et al. 2011; Kong et al. 2011; Chen et al. 2012a, b). However, the lake level elevations and areas of QTP lakes for a specific period (such as the Holocene) are poorly known due to insufficient dating of the shoreline deposits that cover most regions of the QTP. Improvements in the optically stimulated luminescence (OSL) dating method, such as use of the single aliquot regeneration (SAR) protocol (Murray and Wintle 2000), has led to a rapid increase in the number of date shorelines on the QTP (Madsen et al. 2008; Lee et al. 2009; Fan et al. 2010; Li et al. 2009; Liu et al. 2010, 2011; Rhode et al. 2010; Xue et al. 2010; Chen et al. 2012b; Long et al. 2012; Pan et al. 2012).

In this study, we investigate shorelines of QTP lakes that formed during the last lake regression phase using Google Earth and 30-m-resolution Aster-DEM (downloaded from: <http://datamirror.csdb.cn>), together with published shoreline chronologies, to explore Holocene lake elevation and area variations. We then discuss possible causes of regional differences in lake elevation and area responses.

### Shorelines on the QTP during the regressive phase

The origin of QTP lakes is the result of tectonic uplift of the QTP and of the uplift of mountain ranges and the sinking of basins on it (Chen 1981; Chen and Lin 1993). Based on satellite interpretation, Chen and Lin (1993)

proposed there were two main periods of lake expansion and contraction on the QTP: an early one that occurred during the early Pleistocene, and a later one that occurred during the late middle Pleistocene. Chen (1986) found that the QTP lakes responded differently to these lake cycles, with those in the southern portion of northern Tibet shrinking markedly, those in the northwestern and southern portions of Tibet lakes retreating moderately, and those in northernmost Tibet shrinking only slightly. This lake evolution process contrasts with the modern precipitation distribution pattern on the QTP in which rainfall amounts decrease across a southeastern to northwestern gradient. He contributes this phenomenon to differential lake sizes and to catchment geomorphological processes (Chen 1986). Li (2000) found the highest lake levels during the last lake cycle were variable for different regions of the QTP. The highest lake levels occurred in the central and western Qiangtang Plateau, moderately high lake level occurred in the northeastern Qiangtang Plateau and southernmost QTP, while the lowest high lake levels occurred in the eastern QTP (Li 2000). Hudson et al. (2011) also found that the height of paleoshorelines above modern lake levels was higher in the western QTP than on the eastern side.

In this study, we investigated the height differentials between the highest continuous paleoshorelines and modern lake levels for a series of lakes on the QTP. Lakes with an area greater than 40 km<sup>2</sup> were selected because paleoshorelines around these lakes are clear and easy to identify, and because lakes smaller than 40 km<sup>2</sup> are too numerous (more than 1,000 on the QTP). We then identified the highest continuous shoreline around each lake using Google Earth and made sure this shoreline had a clear shoreline morphology, was spatially extensive, and was found around the entire lake. Finally, we vectorized this highest continuous shoreline in Google Earth, exported and loaded the file in Arcgis 9.2 with Aster-DEM as a basemap, and obtained the elevation of the highest continuous shoreline. These baseline data were obtained for 127 lakes on the QTP (Fig. 1). We tested these results by conducting field leveling surveys and by using differential global positioning system (dGPS) measurements of the height between the highest continuous shorelines and modern lake levels of Qinghai Lake, Serling Co, and Bangong Co, and found them to be generally in consistent with Google Earth and Aster-DEM derived results within 3-m variation. We therefore feel confident in combining Google Earth and 30-m-resolution Aster-DEM data to obtain the altitudes of the highest continuous shorelines and the modern lake levels for the remaining lakes.

Most lakes on the QTP are located in the Gangdise, Qiangtang, west Holxil-Yushu, and northeastern QTP areas (Fig. 1). The height differential between the highest continuous shoreline and present lake level was divided into 4

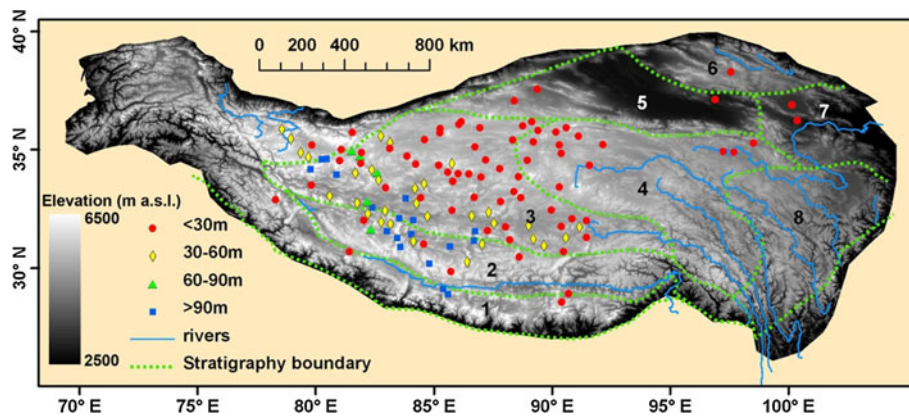


**Fig. 1** Distribution of lakes on the Qinghai-Tibetan Plateau showing the height of the highest continuous shorelines above present lake surfaces using a Digital Elevation Model base map. *Green dashed lines* represent stratigraphic block boundaries (modified from: Zhang

et al. 2008): 1 Yarlung Zangbo-Himalayan area; 2 Gangdise area; 3 Qiangtang area; 4 Holxil-Yushu area; 5 Qaidam area; 6 Jiuquan-Zhangye area; 7 Xining-Lanzhou area; 8 Western Sichuan-Eastern Tibet area

groups: lower than 30, 30–60, 60–90 m, and higher than 90 m. The lakes with 30–60, 60–90 m, and higher than 90-m differentials are distributed in a northwestern-to-southeastern trend line, covering the central and western Gangdise and southern/southwestern Qiangtang areas (Fig. 1). Lakes with differentials lower than 30 m dominate the eastern Qiangtang, Holxil-Yushu, Yalung zangbo-Himalayan, and northeastern QTP areas (Fig. 1). Lakes with differentials of 60–90 m and higher than 90 m are all located west of longitude 87°E (Fig. 1). These differences are difficult to explain by topographical factors, as lakes in these areas with differentials of 30–60, 60–90 m, and higher than 90 m are located mainly in relatively flat areas and do not differ topographically from lakes with differentials lower than 30 m located in flat areas of QTP such as the Holxil, Qaidam basins (Fig. 2).

### Holocene lake level variations of the QTP

A number of papers using U-series, OSL, and cosmogenic  $^{10}\text{Be}$  and  $^{26}\text{Al}$  dating to establish paleoshoreline chronologies on the QTP have been published in the past few

decades. However, the high lake level stages of the QTP remain poorly understood and the magnitude of regional differences is still unclear due to a lack of sufficient and reliable paleoshoreline chronologies. In this study, we analyzed 12 lakes from different regions of the QTP that have established Holocene paleoshoreline chronologies (Fig. 3). Based on these chronologies, we investigated lake level heights, lake areas, and water volumes more than present for shorelines higher than at present.

The lakes in our study with Holocene shoreline chronologies are the Qinghai Lake (Liu 2011), Dalianhai Lake (Chen et al. 2012a), Linggo Co (Pan et al. 2012), Serling Co (Li et al. 2009; Xue et al. 2010), Tangqung Co (Kong et al. 2011), Tangra Yumco (Long et al. 2012), Zhari Namco (Chen et al. 2012b), Drolung Co (Kong et al. 2011), Lagkor Co (Lee et al. 2009), Chabyer Caka (Hudson and Quade 2013), Ngangla Ringco (Hudson et al. 2011; Hudson and Quade 2013), and Sumxi and Longmu Co (Kong et al. 2007) (Fig. 3). The locations, modern lake level altitudes, and lake areas of these lakes are listed in Table S1, while the reported paleoshoreline chronologies for these lakes are listed in Table S2.

**Fig. 2** Distribution of lakes on the Qinghai-Tibetan Plateau showing the height of the highest continuous shorelines above present lake surfaces relative to slope

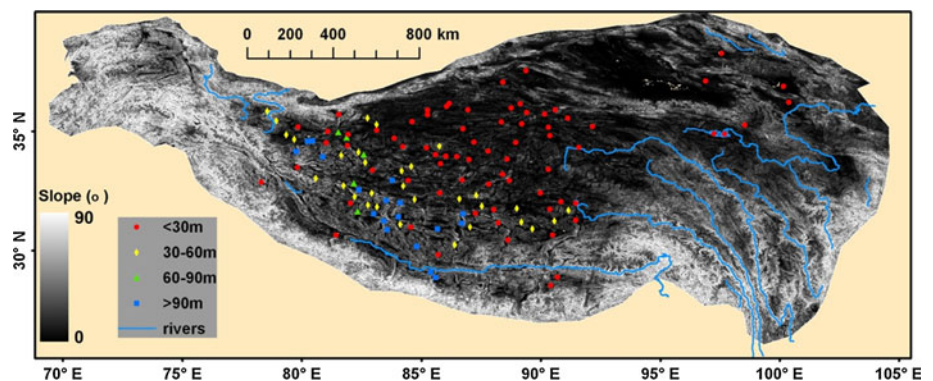
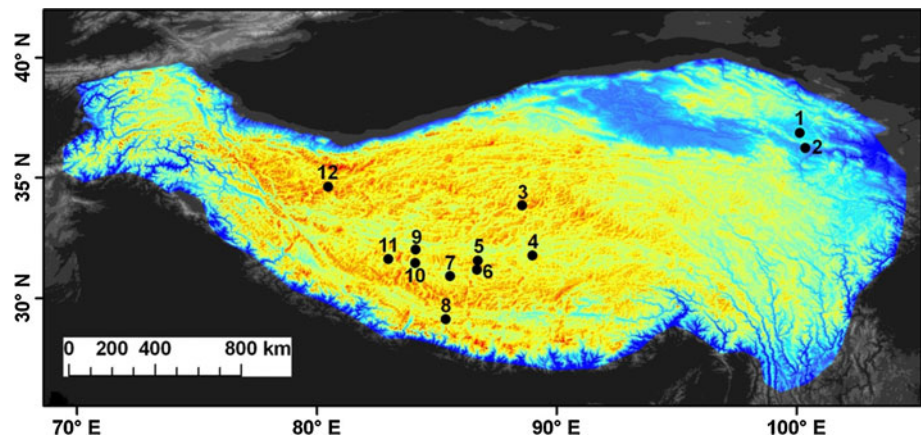


**Fig. 3** Lakes with published Holocene paleoshoreline chronologies used in this study: 1 Qinghai Lake; 2 Dalianhai Lake; 3 Linggo Co; 4 Serling Co; 5 Tangqung Co; 6 Tangra Yumco; 7 Zhari Namco; 8 Drolung Co; 9 Lakgor Co; 10 Chabyer Caka; 11 Ngangla Ringco; 12 Sumxi and Longmu Co



### Qinghai Lake

Qinghai Lake is located on the northeastern QTP and is the largest closed-basin saline lake in China (Fig. 3). The lake level was 3,193.4 m above sea level (a.s.l.) in March 2010 (Liu et al. 2011). Liu (2011) reconstructed lake level variation histories of Qinghai Lake since the last interglacial based on the OSL dating of paleoshoreline sediments. The highest Holocene lake level ( $\sim 10.9$  m above present) persisted from 8 to 6 ka (Liu 2011). For this study, we select the 4 high Holocene lake level stages (8, 6, 1.77, and 0.32 ka).

### Dalianhai Lake

Dalianhai Lake is located in the Gonghe basin, on the northeastern QTP (Fig. 3). The lake level elevation was 2,855 m in the 1980s, but the lake has dried out since 1994 when its main tributary was dammed. Calibrated  $^{14}\text{C}$  ages of the shorelines indicate that the lake level was 2,860 and 2,870 m at 1.3 and 11.4 ka BP (before present, present refers to 1950), respectively (Chen et al. 2012a).

### Linggo Co

Linggo Co lies in the eastern portion of the Qiangtang area (Figs. 1, 3), is elongated in an S–N direction, and has a surface area of 100 km<sup>2</sup>, and the present lake surface elevation is 5,059 m a.s.l. (Pan et al. 2012). Linggo Co has paleoshorelines at 6, 4, and 1 m above the present lake level. OSL ages for these levels are 9.6 ka for the 6 m level, 9, 6.1, and 1.9 ka for the 4 m level, and 3.1 and 0.9 ka for the 1 m level (Pan et al. 2012).

### Serling Co

Serling Co, located in the Qiangtang area (Figs. 1, 3), is the second largest lake in the central QTP and has a present

lake level altitude of 4,544 m (Li et al. 2009). Li et al. (2009) reported OSL chronologies indicating paleoshorelines 40, 31, and 10 m above the present lake formed at 9.6, 9.2, and 6.9 ka, respectively, while OSL ages reported by Xue et al. (2010) on paleoshorelines 17, 12, and 10 m above the present lake formed at 12.2, 6.3, and 2.3 ka, respectively.

### Tangqung Co

Tangqung Co is located in the southern Qiangtang area (Figs. 1, 3), in Nima County at an elevation of 4,469 m a.s.l. (Kong et al. 2011). Paleoshorelines at altitudes of 4,710 and 4,476 m altitude were dated to be 8.7 and 2.2 ka, respectively, by cosmogenic  $^{10}\text{Be}$  and  $^{26}\text{Al}$  dating (Kong et al. 2011).

### Tangra Yumco

Tangra Yumco is located to the south of the Tangqung Co in Nima County at an elevation of 4,535 m a.s.l. (Kong et al. 2011) (Fig. 3). One exposed profile, composed of shallow water sediments, deep water sediments, and shoreline deposits (top to bottom), was located at  $\sim 25$  m above the present lake surface (Long et al. 2012). Three OSL dates of 7.6, 3.4, and 2.3 ka were obtained from the uppermost, middle, and lowermost deep water sediments, respectively (Long et al. 2012).

### Zhari Namco

Zhari Namco is located near the boundary between the Qiangtang and Gangdise areas (Figs. 1, 3), at an elevation of 4,616 m. Chen et al. (2012b) dated paleoshorelines that are 128, 94, 80, 64, 22, and 14 m above the present lake level using OSL (Table S2). The chronologies of these paleoshorelines are 8.2, 5.4, 4.7, 3.8, 2.1, and 0.7 ka, respectively (Chen et al. 2012b).

### Drolung Co

Drolung Co is located in the northern portion of the Yarlung Zangbo-Himalayan area (Figs. 1, 3) at an elevation of 4,600 m (Kong et al. 2011). Two paleoshorelines that are 100 and 87 m above the present lake were dated to be 3.7 and 3.9 ka, respectively, by cosmogenic  $^{10}\text{Be}$  and  $^{26}\text{Al}$  dating (Kong et al. 2011).

### Lagkor Co and Chabyer Caka

Lagkor Co, located in the southern Qiangtang area (Figs. 1, 3), is a small hypersaline lake of 95.6 km<sup>2</sup> with a present lake surface of 4,470 m a.s.l. (Lee et al. 2009). Four paleoshorelines at 130, 127, 105, and 74 m above the present lake surface were dated to 5.2, 4.9, 3.7, and 3.2 ka, respectively, by OSL (Lee et al. 2009). Chabyer Caka lies 65 km to the south of Lagkor Co and is a hypersaline lake with a surface area of 256.2 km<sup>2</sup> and a present lake level elevation of 4,429 m (Table S1). At present, Chabyer Caka connects with Taro Co. Lagkor Co, Chabyer Caka, and Taro Co to form a larger lake when lake levels reach higher than ~4,550 m. Two high paleoshorelines at 4,585 and 4,599 m a.s.l. in the adjacent lake system of Chabyer Caka were dated to 11.1 and 9.9 ka, respectively (Hudson and Quade 2013).

### Ngangla Ringco

Ngangla Ringco lies in the central Gangdise area (Figs. 1, 3), at an elevation of 4,721 m (Table S1). Hudson and Quade (2013) report a new lake level chronology based on  $^{14}\text{C}$  dated shoreline tufas (inorganic  $\text{CaCO}_3$ ) from shoreline deposits of Ngangla Ringco. Lake levels rose abruptly at 10.1 ka to a highstand elevation 133 m above the modern lake level, stabilized there until 9.0 ka, and then dropped periodically over the remainder of the Holocene (Hudson et al. 2011).

### Sumxi and Longmu Co

Sumxi Co and Longmu Co are located in the northwestern Qiangtang area (Figs. 1, 3), and the present lake surface elevations of these two lakes are 5,058 and 5,008 m a.s.l. (Kong et al. 2007). When the lake surface exceeds 5,100 m, these two lakes combine to form one single lake (Gasse et al. 1991). Gasse et al. (1991), using  $^{14}\text{C}$  dating, dated paleoshorelines between 5,105 and 5,070 m a.s.l., to between 7.7 and 7.0 ka. However, their dating results for the same samples were not consistent with others (Li 2000). Kong et al. (2007) obtained dated high paleoshoreline of 5,160, 5,149, and 5,145 m to 12.8, 11.3, and 7.8 ka, respectively, using cosmogenic  $^{10}\text{Be}$  dating. In this

study, we use the chronology reported by Kong et al. (2007).

Using Arcgis 9.2, 30-m-resolution Aster-DEM, together with the chronologies and altitudes of the highest Holocene shorelines, we reconstructed the maximum Holocene extensions of these 12 lakes (Fig. 4). During the highest Holocene lake level stage, a big lake containing the Zhari Namco, Dawa Co, Nganggun Co, Qigai Co, Damazi Co, and Monco Bunnyi sub-basins appeared in the central Gangdise area of the southern QTP (Fig. 4b). Tangra Yumco and Tangqung Co also combined to form a larger lake during the highest Holocene lake level stage (Fig. 4f), as did Longmu Co and Sumxi Co (Fig. 4c), Ngangla Ringco, Ringinyubu Co, and Co Nag (Fig. 4g), and Lagkor Co, Chabyer Caka, and Taro Co (Fig. 4i). A large Serling Co formed during the highest Holocene lake level period and included modern Serling Co, Urru Co, Qiagoi Co, Pongce Co, Pangkog Co, and Co Ngoin (Fig. 4j). Drolung Co similarly expanded greatly (Fig. 4e), and when levels exceeded 4,723 m a.s.l., it overflowed into the Yarlung Tsangpo River (Kong et al. 2011). Dalianhai Lake expanded substantially during this period, but only as the result of the flat terrain around the lake (Figs. 2, 4a). The Qinghai Lake and Linggo Co expanded only slightly when compared with other lakes (Fig. 4d, h). Hala Lake, which lies ~100 km northwest of Qinghai Lake, had a Holocene highstand similar to the present lake surface elevation based on drill core data (Wünnemann, et al. 2012).

We also calculated the lake areas and water volumes greater than at present of these 12 lakes for different high lake level stages. Figure 5a shows that the highest Holocene levels of Lakgor Co, Drolung Co, Tangqung Co, Tangra Yumco, Longmu Co, Ngangla Ringco, and Zhari Namco exceeded 100 m higher than present. The highest lake level of Serling Co was 40 m above present lake surface at 9.6 ka (Fig. 5a), while levels of Qinghai Lake, Dalianhai Lake, and Linggo Co were only 10.9, 15, and 6 m, respectively, above the present lake surfaces (Fig. 5a). In all these cases, the highest lake levels occurred during the early Holocene, with lake levels dropping gradually since then (Fig. 5a). The ratios of the areas of the high lake level stages to those of the present lake areas, and lake water volumes greater than at present (Fig. 5b, c), show similar trends. The lake areas were bigger, and lake water volumes were larger than at present during the early Holocene, then gradually decreased through the middle and late Holocene (Fig. 5b, c). The anomalous trend of lake area of Lagkor Co in Fig. 5b was due to the disintegration of the larger lake after 3.7 ka, leading to the separate evolution of Lagkor Co.

The highest Holocene paleoshorelines of Lagkor Co, Chabyer Caka, Drolung Co, Tangra Yumco, Tangqung Co, Zhari Namco, Sumxi and Longmu Co, Ngangla Ringco,

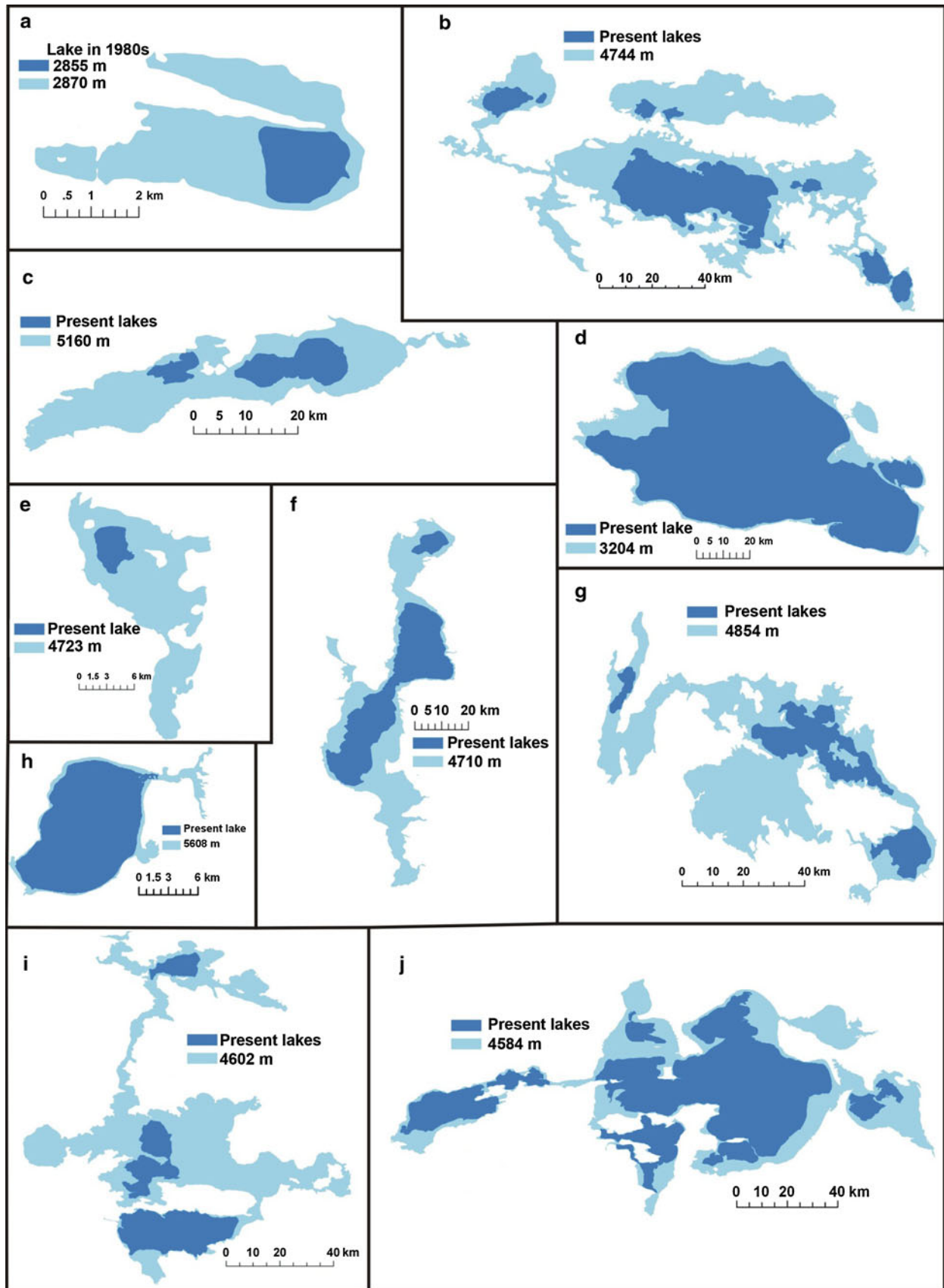


**Fig. 4** Lake extensions for both the modern and highest Holocene shoreline for lakes used in this study: **a** Dalianhai Lake; **b** Zhari Namco; **c** Sumxi and Longmu Co; **d** Qinghai Lake; **e** Drolung Co; **f** Tangqung Co and Tangra Yumco; **g** Ngangla Ringco; **h** Drolung Co; **i** Lakgor Co and Chabyer Caka; **j** Serling Co

Serling Co, Linggo Co, and Dalianhai Lake are close to the highest continuous shorelines around these lakes. These lakes lie in the region of lakes with a >90-m differential between highest and present shorelines in Fig. 1. By combining reported age estimates with the elevations of the highest continuous shorelines, we propose that the shorelines that were formed during the last transgressive/regressive cycle, have a clear shoreline morphology, and are spatially extensive were formed during the Holocene. Those shorelines formed before the Holocene were extensively reworked by later geomorphological processes. Hudson and Quade (2013) also suggested that the highest continuous shorelines around lakes in the southern QTP are early Holocene in age.

Figures 1 and 2 show the magnitude of Holocene lake level variations in different regions of the QTP. During periods of Holocene high lake levels some lakes in the southern and southwestern QTP were combined into larger lakes, but separated when environmental conditions gradually deteriorated. The height differentials between Holocene highstands and modern lake levels decreases from the central Gangdise and southern/southwestern Qiangtang areas to the eastern Qiangtang, Holxil-Yushu, Yalung Zangbo-Himalayan, and northeastern QTP areas (Fig. 1). For lakes located more closer to the interior QTP, the amplitude of the lake level fluctuation is more smaller (Fig. 1).

Fan (1983) defined the water supply coefficient as the ratio of watershed area to lake area, and proposed that the water supply coefficient of closed-basin lakes on the QTP reflects the relative effective moisture conditions of their drainage basins. He found that the water supply coefficient of the inland closed-basin lakes on the QTP increased from south to north and from southeast to northwest. This suggests that small drainage basin on the southern and southeastern QTP could maintain relative large lakes, while much larger drainage basins are needed on the northern and northwestern QTP in order to maintain the same-sized lakes. This is consistent with modern precipitation distribution patterns that reflect a decrease in precipitation from the southeast to the northwest on the QTP. Figure 6 shows the ratios of lake areas to drainage basin areas (reverse to the water supply coefficient) of Lagkor Co, Zhari Namco, Serling Co, and Qinghai Lake during the Holocene. During the early Holocene, the areas of Lagkor Co and Zhari Namco are in excess of 20 % of their drainage basin area, Serling Co reached 13.7 % of its drainage basin area, and Qinghai Lake reached 16.6 % of its drainage basin area

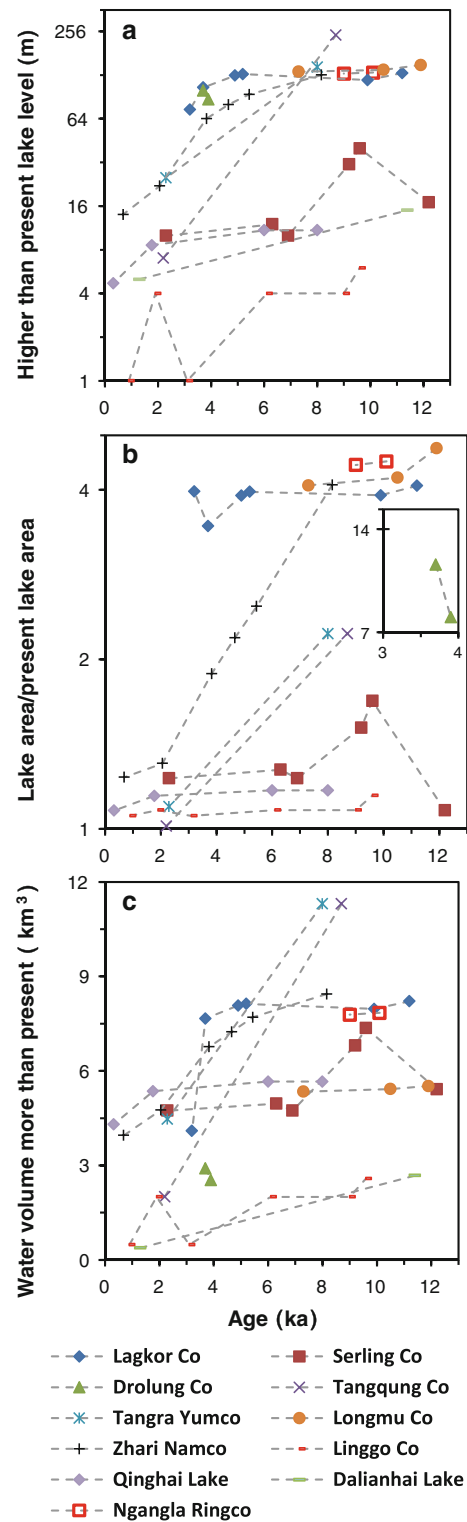


**Fig. 5** Lake level, lake area, and water volume variations for lakes discussed in this study: **a** height above present lake surface during the Holocene highstands; **b** ratios of modern lake areas to those of Holocene highstands (The ordinate axis is a logarithmic scale); **c** water volumes more than present (WVMP) during Holocene highstands. In order to illustrate clearly, the values for ordinate axis were calculated by formula  $\text{Log}_2^{(\text{WVMP} \cdot 10)}$  for Dalianhai Lake and Tangqung Co,  $\text{Log}_2^{(\text{WVMP} \cdot 100)}$  for Linggo Co, and  $\text{Log}_2^{(\text{WVMP})}$  for other lakes

(Fig. 6). Thereafter, the ratio of lake area to drainage basin area decreased steadily for Lagkor Co, Zhari Namco, and Serling Co, but decreased only slightly for Qinghai Lake (Fig. 6). This implies that the water supply changed substantially after the early Holocene, causing lake levels, areas, and water volumes to decline to their present states.

### The driving mechanism of Holocene QTP lake level variations

On average, summer precipitation brought by Asian Summer Monsoon (ASM) constitutes 60–80 % of the annual precipitation in QTP (Lu et al. 2007). Modern meteorological observations show that most summer precipitation in mainland China is derived from the Indian Ocean (Clemens et al. 2010). An et al. (2000) proposed that in southwestern China the peak post-glacial summer precipitation occurred ~11 ka ago and was probably related to the maximum landward extension of the Indian Summer Monsoon (ISM). Wang et al. (2010) support previous observations that climate evolution in monsoon central Asia since the last glacial roughly paralleled changes in northern hemisphere summer insolation. The ISM area exhibits maximum wet conditions during the early Holocene (Wang et al. 2010). The ASM (consisting of both ISM and EASM) is controlled mainly by a land–ocean surface thermal contrast, with surface heating on the QTP being important for generating orographic air ascent (Wu et al. 2012). The middle latitude (30°N) summer solar insolation of the Northern Hemisphere decreased continuously during the Holocene (Fig. 7a). The ASM began to be enhanced following the last deglaciation, reached its high point during the early Holocene, and then weakened gradually

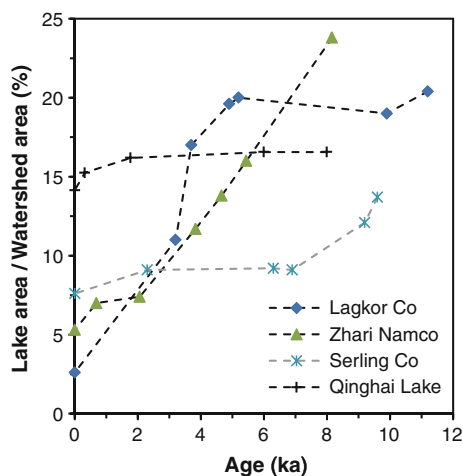


**Fig. 6** Ratios of lake areas to drainage basin areas for four QTP lakes during Holocene highstands

through the middle to the late Holocene (Fig. 7c–f). An integrated QTP precipitation curve (Hou et al. 2012) shows that precipitation was highest during the early Holocene and declined gradually thereafter (Fig. 7b). Oxygen isotope values from the Guliya ice core were positive between 12 and 6 ka and rapidly became negative at ~6 ka (Fig. 7g), implying a significant environmental change occurred. The strong early Holocene ASM is contemporaneous with the highest Holocene QTP lake levels, and the subsequent weakening of the ASM is contemporaneous with QTP lake regressions. The parallel shifts in Northern Hemisphere middle latitude solar insolation, ASM, and QTP lake level variations suggest insolation changes were the forcing mechanism behind QTP climate change and lake level fluctuations. The direct link may be that higher solar insolation enhanced heating of the Plateau drawing more moisture laden air to the higher elevations of the QTP (Wu et al. 2012). Hudson and Quade (2013) suggest that the paleoshorelines of early Holocene paleolakes on Tibet were related to increased precipitation brought by intensified Asian monsoon and that ISM rainfall increased much

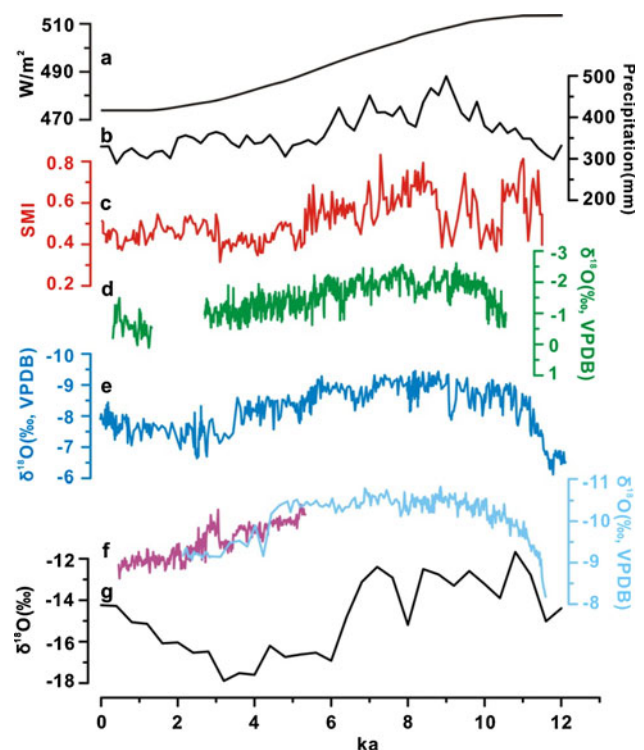


**Fig. 7** Climate proxy records related to Holocene climate change on the QTP: **a** summer solar insolation at 30°N during the Holocene (Berger and Loutre 1991); **b** reconstructed Holocene precipitation on the QTP (Hou et al. 2012); **c** summer monsoon index from Qinghai Lake (An et al. 2012); **d**  $\delta^{18}\text{O}$  values from the Oman Stalagmite (Fleitmann et al. 2003); **e**  $\delta^{18}\text{O}$  values from the Dongge Cave Stalagmite (Dykoski et al. 2005); **f**  $\delta^{18}\text{O}$  values from the Sanbao Cave Stalagmite (Wang et al. 2008); **g**  $\delta^{18}\text{O}$  values from the Guliya ice core (Thompson et al. 1997)

more than EASM rainfall in Tibet during the early Holocene wet period. However, it is worth noting that while lake level variations were primarily related to climate change, they were also affected by regional tectonic movements, basin topography, watershed size, lake size, and even the glaciers within the lake basin.

## Conclusions

In this study, we investigated the spatial distribution of high lake levels on the QTP during the last lake cycle and explored the process of Holocene lake evolution using published paleoshoreline chronologies, Google Earth, Aster-DEM, and Arcgis 9.2 software. We concluded that (1) the paleoshorelines of last major lake cycle were formed during the Holocene; (2) as the lakes located more closer to the interior QTP, the amplitude of the lake level fluctuation is more smaller; (3) the high lake levels were probably due to Northern Hemisphere solar insolation forcing. More paleoshoreline chronologies are needed to more completely understand lake evolution processes on the QTP.

**Acknowledgments** This study was financially supported by China NSF Grant #41201014, the Open Research Fund of Key Laboratory of Tibetan Environmental Changes and Land Surface Processes, Chinese Academy of Sciences (CAS), the West Doctor fund of West Light program of CAS, and the postdoc fund Qinghai Institute of Salt Lakes given to X.-J. Liu. The constructive comments made by two anonymous reviewers helped greatly to improve the manuscript. Thanks to professor S.-H. Li created chance for me to study in the HKU, that prompted the accomplishment of this study.

## References

- An ZS, Porter SC, Kutzbach JE, Wu XH, Wang SM, Liu XD, Li XQ, Zhou WJ (2000) Asynchronous Holocene optimum of the East Asian monsoon. *Quat Sci Rev* 19:743–762
- An ZS, Colman SM, Zhou WJ, Li XQ, Brown ET, Timothy Jull AJ, Cai YJ, Huang YS, Lu XF, Chang H, Song YB, Xu H, Liu WG, Jin ZD, Liu XD, Cheng P, Liu Y, Ai L, Li XZ, Liu XJ, Yan LB, Shi ZG, Wang XL, Wu F, Qiang XK, Dong ZB, Lu FY, Xu XW (2012) Interplay between the Westerlies and Asian monsoon recorded in Lake Qinghai sediments since 32 ka. *Sci Rep*. doi: [10.1038/srep00619](https://doi.org/10.1038/srep00619)
- Avouac JP, Dobremez JF, Bourjot L (1996) Paleoclimatic interpretation of a topographic profile across middle Holocene regressive shorelines of Longmu Co (Western Tibet). *Palaeogeogr Palaeoclimatol Palaeoecol* 120:93–104
- Berger A, Loutre MF (1991) Insolation values for the climate of the last 10 million years. *Quat Sci Rev* 10:297–317
- Chen ZM (1981) The origin of lakes on Xizang Plateau. *Oceanologia ET Limnologia Sinica* 12:178–187 (In Chinese with English abstract)
- Chen ZM (1986) Lake retreat in Qinghai-Xizang Plateau with additional reference to its climatic significance. *Oceanologia ET Limnologia Sinica* 17:207–216 (In Chinese with English abstract)
- Chen ZE, Lin QY (1993) Significance of neotectonic movement of lake extension and shrinkage in Qinghai-Tibet Plateau. *Earthquake* 1:31–40 (In Chinese with English abstract)
- Chen FH, Zhang JW, Cheng B, Yang TB (2012a) Late Quaternary high lake levels and environmental changes since last deglacial in Dalianha, Gonghe Basin in Qinghai Province. *Quat Sci* 32:123–132 (In Chinese with English abstract)
- Chen YW, Li SH, Zong YQ (2012b) Holocene lake level variations of Zhari Namco (submitted)
- Clemens SC, Prell WL, Sun YB (2010) Orbital-scale timing and mechanisms driving Late Pleistocene Indo-Asian summer monsoons: reinterpreting cave speleothem  $\delta^{18}\text{O}$ . *Paleoceanography* 25: PA4207. doi: [10.1029/2010PA001926](https://doi.org/10.1029/2010PA001926)
- Dykoski CA, Edwards RL, Cheng H, Yuan DX, Cai YJ, Zhang ML, Lin YS, Qing JM, An ZS, Revenaugh J (2005) A high-resolution, absolute-dated Holocene and deglacial Asian monsoon record from Dongge Cave, China. *Earth Planet Sci Lett* 233:71–86
- Fan YQ (1983) The supply coefficient of interior lakes in Xizang. *Oceanologia ET Limnologia Sinica* 14:117–127 (In Chinese with English abstract)
- Fan QS, Lai ZP, Long H, Sun YJ, Liu XJ (2010) OSL chronology for lacustrine sediments recording high stands of Gahai Lake in Qaidam Basin, northeastern Qinghai-Tibetan Plateau. *Quat Geochronol* 5:223–227
- Fleitmann D, Burns SJ, Mudelsee M, Neff U, Kramers J, Mangini A, Matter A (2003) Holocene forcing of the Indian monsoon recorded in a stalagmite from southern Oman. *Science* 300:1737–1739
- Fontes JC, Gasse F, Gibert E (1996) Holocene environmental changes in Lake Bangong basin (Western Tibet). Part 1: chronology and stable isotopes of carbonates of a Holocene lacustrine core. *Palaeogeogr Palaeoclimatol Palaeoecol* 120:25–47
- Gasse F, Arnold M, Fontes JC (1991) A 13000 year climate record from western Tibet. *Nature* 353:742–745
- Hou GL, Chongyi E, Xiao JY (2012) Synthetical reconstruction of the precipitation series of the Qinghai-Tibet Plateau during the Holocene. *Prog Geogr* 31:1–7 (In Chinese with English abstract)
- Hudson AM, Quade J (2013) Long-term east-west asymmetry in monsoon rainfall on the Tibetan Plateau. *Geology* 41:1–4
- Hudson AM, Quade J, Lei G (2011) Shores of Tibet: history of changing lake levels across the Tibetan Plateau. AGU fall meeting (Bibliographic Code: 2011AGUFMGC11D..06H)
- Jia YL, Shi YF, Wang SM, Jiang XZ, Li SJ, Wang AJ, Li XS (2001) Lake expanding events in the Tibetan Plateau since 40 ka BP. *Sci China (Ser D)* 44:301–315
- Kong P, Na CG, Fink D, Huang FX, Ding L (2007) Cosmogenic  $^{10}\text{Be}$  inferred lake-level changes in Sumxi Co basin, Western Tibet. *J Asian Earth Sci* 29:698–703
- Kong P, Na CG, Brown R, Fabel D, Freeman S, Xiao W, Wang YJ (2011) Cosmogenic  $^{10}\text{Be}$  and  $^{26}\text{Al}$  dating of paleolake shorelines in Tibet. *J Asian Sci* 41:263–273
- Lee J, Li SH, Aitchison JC (2009) OSL dating of paleoshorelines at Lagkor Tso, western Tibet. *Quat Geochronol* 4:335–343
- Li BY (2000) The last greatest lakes on the Tibetan Plateau. *Acta Geographica Sinica* 55:174–182 (In Chinese with English abstract)
- Li BY, Wang SM, Zhu LP, Li YF (2001) 12 ka BP lake environment on the Tibetan Plateau. *Sci China (Series D)* 44:324–331
- Li DW, Li YK, Ma BQ, Dong GC, Wang LQ, Zhao JX (2009) Lake-level fluctuations since the last Glaciation in Selin Co (lake), Central Tibet, investigated using optically stimulated luminescence dating of beach ridges. *Environ Res Lett* 4:1–10
- Liu XJ (2011) The late quaternary lake level history of Qinghai lake based on quartz optically stimulated luminescence. Dissertation,

- Qinghai Institute of Salt Lakes, Chinese Academy of Sciences (In Chinese with English abstract)
- Liu XJ, Lai ZP, Fan QS, Long H, Sun YJ (2010) Timing for high lake levels of Qinghai Lake in the Qinghai-Tibetan Plateau since the last interglaciation based on quartz OSL dating. *Quat Geochronol* 5:218–222
- Liu XJ, Lai ZP, Yu LP, Liu K, Zhang JR (2011) Lake level variations of Qinghai Lake in northeastern Qinghai-Tibetan Plateau since 3.7 ka based on OSL dating. *Quat Int* 236:57–64
- Long H, Lai ZP, Frenzel P, Fuchs M, Haberzettl T (2012) Holocene moist period recorded by the chronostratigraphy of a lake sedimentary sequence from Lake Tangra Yumco on the south Tibetan Plateau. *Quat Geochronol* 10:136–142
- Liu HL, Shao QQ, Liu JY, Wang JB, Chen ZQ (2007) Temporo-spatial distribution of summer precipitation over Qinghai-Tibet Plateau during the last 44 years. *Acta Geographica Sinica* 62:946–958 (In Chinese with English abstract)
- Madsen DB, Ma HZ, Rhode D, Brantingham PJ, Forman SL (2008) Age constraints on the late Quaternary evolution of Qinghai Lake, Tibetan Plateau. *Quat Res* 69:316–325
- Meng K, Shi XH, Wang EQ, Su Z (2012) Geomorphic characteristics, spatial distribution of paleoshorelines around the Siling Co area, Central Tibetan Plateau, and the lake evolution within the Plateau. *Chin J Geol* 47:730–745 (In Chinese with English abstract)
- Murray AS, Wintle AG (2000) Luminescence dating of quartz using an improved single-aliquot regenerative-dose protocol. *Radiat Meas* 32:53–57
- Pan BL, Yi CL, Jiang T, Dong GC, Hu G, Jin Y (2012) Holocene lake-level changes of Linggo Co in central Tibet. *Quat Geochronol* 10:117–122
- Rhode D, Ma HZ, Madsen DB, Brantingham PJ, Forman SL, Olsen JW (2010) Paleoenvironmental and archaeological investigation at Qinghai Lake, western China: geomorphic and chronometric evidence of lake level history. *Quat Int* 218:29–44
- Shi YF, Liu XD, Li BY, Yao TD (1999) A very summer monsoon event during 30–40 ka BP in the Tibetan Plateau and the relation to precessional cycle. *Chin Sci Bull* 44:1475–1480
- Shi YF, Yu G, Liu XD, Li BY, Yao TD (2001) Reconstruction of the 30–40 ka BP enhanced Indian monsoon climate based on geological records from the Tibetan Plateau. *Palaeogeogr Palaeoclimatol Palaeoecol* 169:69–83
- Stapor FW (1982) Beach ridges and beach ridge coasts: encyclopedia of beaches and coastal environments. Hutchinson Ross, Stroudsburg, PA, pp 160–161
- Tamura T (2012) Beach ridges and prograded beach deposits as palaeoenvironment records. *Earth Sci Rev* 114:279–297
- Thompson LG, Yao TD, Davis ME, Henderson KA, Thompson EM, Lin PN, Beer J, Synal HA, Dai JC, Bolzan JF (1997) Tropical climate instability: the last glacial cycle from a Qinghai-Tibetan ice core. *Science* 276:1821–1825
- Wang SM, Shi YF (1992) Review and discussion on the late Quaternary evolution of Qinghai Lake. *J Lake Sci* 4:1–9 (In Chinese with English abstract)
- Wang YJ, Cheng H, Edwards RL, Kong XG, Shao XH, Chen ST, Wu JY, Jiang XY, Wang XF, An ZS (2008) Millennial- and orbital-scale changes in the East Asian monsoon over the past 224000 years. *Nature* 451:1090–1093
- Wang YB, Liu XQ, Herzschuh U (2010) Asynchronous evolution of the Indian and East Asian Monsoon indicated by Holocene moisture patterns in monsoonal central Asia. *Earth Sci Rev* 103:135–153
- Wu GX, Liu YM, He B, Bao Q, Duan AM, Jin FF (2012) Thermal controls on the Asian summer monsoon. *Scientific Rep.* doi: [10.1038/srep00404](https://doi.org/10.1038/srep00404)
- Wünnemann B, Wagner J, Zhang YZ, Yan DD, Wang R, Shen Y, Fang XY, Zhang JW (2012) Implications of diverse sedimentation patterns in Hala Lake, Qinghai Province, China for reconstructing Late Quaternary climate. *J Paleolimnol.* doi: [10.1007/s10933-012-9641-2](https://doi.org/10.1007/s10933-012-9641-2)
- Xue L, Zhang ZQ, Liu WM, Lü TY, Sun JM (2010) The shrinking of Siling Co in the past 12 ka-based on OSL dating of past shorelines. *Chin J Geol* 45:1–12 (In Chinese with English abstract)
- Yang JF, Lu SW, Zhao H, Cui XF, Lu XH (2006) Lacustrine sediments' U-seires age and its significance in Jiezechaka lake of Tibet. *J Earth Sci Environ* 28:6–10 (In Chinese with English abstract)
- Zhang KX, Wang GC, Cao K, Liu C, Xiang SY, Hong HL, Kou XH, Xu YD, Chen FN, Meng YN, Chen RM (2008) Cenozoic sedimentary records and geochronological constraints of differential uplift of the Qinghai-Tibet Plateau. *Sci China (Ser D)* 51:1658–1672
- Zhao XT, Zhu DG, Yan FH, Wu ZL, Ma ZB, Mai XS (2003) Climatic change and lake level variation of Nam Co, Xizang since the last interglacial stage. *Quat Sci* 23:41–52 (In Chinese with English abstract)
- Zheng MP, Yuan HR, Zhao XT, Liu XF (2006) The Quaternary Pan-lake (Overflow) period and paleoclimate on the Qinghai-Tibet Plateau. *Acta Geologica Sinica* 80:169–180 (In Chinese with English abstract)
- Zhu DG, Meng XG, Zhao XT, Shao ZG, Ma ZB, Yang CB, Wu ZH, Wang JP (2005) Sedimentary evolution of the Nam Co basin, Tibet, Since 116 ka BP and Qinghai-Tibet Plateau Uplift. *J Geomech* 11:172–180 (In Chinese with English abstract)